Rare earth fluorescence in NASICON type phosphate glass, $Na_3TiZnP_3O_{12}$

G VIJAYA PRAKASH, P NACHIMUTHU, M VITHAL[†] and R JAGANNATHAN*

School of Chemistry, University of Hyderabad, Hyderabad 500 046, India
[†]Department of Chemistry, Osmania University, Hyderabad 500 007, India

Abstract. The emission spectra of Pr^{3+}, Eu^{3+} and Dy^{3+} doped in NASICON type phosphate glass, $Na_3TiZnP_3O_{12}$ (NTZP) are studied. The dopant rare earth ions occupy sites with 8–9 coordination in a highly covalent environment. For Pr^{3+} ion, calculated and observed branching ratios for lasing transitions $^3P_0 \rightarrow {}^3H_{4,6}$ agree well and found to be 0·64 and 0·24, respectively. The emissions of Pr^{3+} show strong temperature dependence on account of Boltzmann population of the higher excited states at room temperature. The excitation spectrum of Eu^{3+} gives rise to phonon assisted side band for $^5D_2 \leftarrow {}^7F_0$ transition at higher energy side with a phonon energy maximum of 1022 cm^{-1} and an electron phonon coupling strength (g) of 0·018. The value of phonon energy maximum agrees with infrared spectral data. The results show that observation of high energy emissions in phosphate glasses require much higher g values. The red/orange and yellow/blue transitions of Eu^{3+} and Dy^{3+}, respectively show that the Eu^{3+} occupy more distorted site than Dy^{3+}.

Keywords. Rare earths; emission spectra; excitation spectra; phonon side band; electron phonon coupling strength; branching ratio.

1. Introduction

Optical studies of rare earth ions in glass systems are of considerable interest due to their potential applications in lasing materials, holographic gratings and hole burning devices (Durville *et al* 1987; Caird *et al* 1991; Yzexing 1995; Cho *et al* 1996; Menezes *et al* 1997). Phosphate glasses belonging to the family of NASICON (acronym for the crystalline sodium superionic conductor based on $Na_{1+x}Zr_2P_{3-x}Si_xO_{12}$) attract special attention as they exhibit several features such as preparation of glasses with systematic variation in composition, low value for maximum phonon energy leading to low nonradiative loss during emission and scope for preparing neat glasses by sol–gel route (Hagman and Kierkegaard 1968; Sobha and Rao 1995a, 1996a, b). They have the general formula $A_mB_nP_3O_{12}$, where A is an alkali or alkaline earth metal ion and B is a tri, tetra or pentavalent metal ion (Sobha and Rao 1995b). It would therefore be of interest to investigate site preferences for the dopant rare earth ions in these glass matrices and study their emission properties as influenced by hypersensitivity, covalency, site asymmetry and the local structure. The present paper deals with the fluorescence properties of Pr^{3+}, Eu^{3+} and Dy^{3+} ions doped in $Na_3TiZnP_3O_{12}$ (hereafter NTZP) glass.

2. Experimental

The glass compositions, $Na_3TiZnP_3O_{12}$ (NTZP) and 2 wt% Ln^{3+} (Pr^{3+}, Eu^{3+} and Dy^{3+}), were prepared using stoichiometric amounts of $NH_4H_2PO_4$, TiO_2, ZnO, $NaNO_3$ (Analytical grade) and 2 wt% Ln_2O_3 (Indian Rare Earths Limited or Aldrich Chemical Co., USA) as starting materials by standard melt quenching procedure. The absorption spectra were recorded on a JASCO 7800 UV-VIS spectrophotometer and Hitachi 3310 spectrophotometer using undoped glass as reference. The excitation and emission spectra were recorded on a Hitachi 3010 spectrofluorimeter using appropriate filters. Densities were measured by Archemedes principle using toluene as immersion liquid. Refractive index measurements were carried out by Brewster angle setup consisting of He–Ne laser and a diode detector. Density (d) and refractive index (η) of the present glass were found to be $3·18 \pm 0·04$ g·cm^{-3} and $1·660 \pm 0·002$, respectively.

3. Results

From the absorption spectra of 2 wt% Pr^{3+} and Dy^{3+} doped in NTZP glass samples, oscillator strengths of the observed transitions were obtained by the area method (table 1) (Carnall *et al* 1978). The Judd–Ofelt parameters ($\Omega_{\lambda = 2,4,6}$) are evaluated from the oscillator strengths of the observed transitions using the procedure described

---

*Author for correspondence

Table 1. Observed and calculated oscillator strengths for Pr^{3+} and Dy^{3+} ions in NTZP glass.

Pr^{3+} transition from $^3H_4$	Energy (cm^{-1})	P(10^{-6})		Dy^{3+} transition from $^6H_{15/2}$	Energy (cm^{-1})	P(10^{-6})	
		obs	cal			obs	cal
$^3F_2$	5197	2·87	2·56	$^4G_{11/2}$*	23596	0·31	0·34
$^3F_3$	6554	5·05	6·17	$^4I_{15/2}$*	22109	0·70	0·43
$^3F_4$	7092	1·56	3·66	$^4F_{9/2}$	21168	0·44	0·23
$^1G_4$	9038	0·50	0·28	$^6F_{3/2}$	13324	0·20	0·17
$^1D_2$	16926	1·41	1·08	$^6F_{5/2}$	12500	1·16	0·92
$^3P_0$	20734	2·61	2·48	$^6F_{7/2}, ^6H_{7/2}$	11164	1·99	3·18
$^3P_1$	21267	3·58	3·81	$^6F_{9/2}, ^6H_{11/2}$	9259	7·13	6·71
$^3P_2$*	22512	7·47	3·57	$^6H_{9/2}, ^6F_{11/2}$*	8032	12·71	12·81
				$^6H_{11/2}$	6035	2·83	1·44
		rms = 1·62				rms = 0·64	

*Hypersensitive.

Table 2. Judd–Ofelt parameters for Pr^{3+} and Dy^{3+} ions in NTZP glass.

Lanthanide ion	$\Omega_2(10^{-20}$ cm$^2)$	$\Omega_4(10^{-20}$ cm$^2)$	$\Omega_6(10^{-20}$ cm$^2)$
Pr^{3+}	2·09 ± 0·39 (1·05 ± 1·29)*	3·95 ± 0·53 (3·79 ± 1·83)	3·29 ± 0·47 (5·40 ± 1·83)
Dy^{3+}	7·04 ± 0·85	9·55 ± 0·60	2·06 ± 1·27

*The values in parenthesis are deduced by including hypersensitive transition $^3P_2 \rightarrow ^3H_4$.

earlier (Reisfeld 1975; Srikanth Sarma *et al* 1992; Nachimuthu and Jagannathan 1995a; Vijaya Prakash *et al* 1998). The values thus obtained are shown in table 2 for Pr^{3+} and Dy^{3+} ions. No attempt was made to evaluate the Judd–Ofelt parameters for Eu^{3+} as the number of transitions observed in the absorption spectrum are limited and masked by the absorption edge characteristic of these glasses. The Judd–Ofelt parameters (Ω_λ) are used to calculate radiative parameters, viz. transition probabilities (A), radiative life times (τ_R), branching ratios (β_{cal}) and stimulated emission cross sections (σ_p) using the relevant relationships given in our earlier works and are shown in table 3 (Nachimuthu and Jagannathan 1995a).

The emission spectra of Pr^{3+}, Eu^{3+} and Dy^{3+} are recorded choosing the appropriate excitation wavelengths. Figure 1 shows the emission spectra of Pr^{3+} doped in NTZP at room temperature and 77 K. The emission spectrum of Eu^{3+} doped in NTZP is shown in figure 2 along with the phonon assisted side band observed in the excitation spectrum monitored at $^5D_0 \rightarrow ^7F_2$. Figure 3 shows the

room temperature emission spectrum of Dy^{3+} doped in NTZP. The observed branching ratios are obtained from the relative intensities of the emission transitions. The emission transitions in the near infrared region are assumed to be comparatively negligible. The values of radiative parameters thus obtained are also given in table 3.

4. Discussion

Pr^{3+}: The ground state of $Pr^{3+}(4f^2)$ is $^3H_4$. The Ω_λ values obtained including the oscillator strengths of the hypersensitive transitions lead to large errors. Pr^{3+} ion is known to show exceptional values for the Judd–Ofelt parameters due to hypersensitive transition $^3P_2 \rightarrow ^3H_4$ (Bunvel *et al* 1992). Hence the values, excluding this transition, which are more reliable for comparison and discussion, are also obtained (table 2). Among the Judd–Ofelt parameters, Ω_2 is the most sensitive to the nature of the matrix. Fluoride glasses which give rise to most ionic matrix have the least Ω_2 values ranging from 0·06

to 0·84 (in units of 10^{-20} cm^2), (Bunvel *et al* 1992; Binnemans and Gorller-Walrand 1998). The much higher Ω_2 values obtained for the present glass shows that the phosphate ligands provide highly covalent environment. An alternate procedure of obtaining Judd–Ofelt parameters, Ω_λ using the experimental branching ratios of $^3P_0$ level has been recommended by Bunvel *et al* (1992). This procedure may however introduce errors due to the uncertainties in branching ratios obtained. The Ω_λ values obtained by this method along with the experimental and calculated oscillator strengths are reproduced in appendix. This procedure led to Ω_2 value significantly lower and more characteristic of ionic systems such as fluoride glasses. The values obtained by the earlier procedure which are characteristic of covalent systems such as phosphate glasses may therefore be considered

as more reliable. It is seen from table 3 that the calculated and observed branching ratios for the lasing transitions $^3P_0 \rightarrow {}^3H_{4,6}$ agree quite well showing that the mechanism leading to non-radiative decays are not very much operative unlike in the case of the weak $^3P_0 \rightarrow {}^3F_2$ laser transition. The calculated τ_R values give the upper limits in all the cases as the actual values are influenced by multiphonon relaxation and cross relaxations between the adjacent ions (Bunvel *et al* 1992). The large radiative decay probabilities observed for the $^3P_0 \rightarrow {}^3H_{4,6}$ and $^3P_0 \rightarrow {}^3F_2$ laser transitions for Pr^{3+} are also in order with the strong interaction of rare earth ions with local sites as suggested by the large electron phonon coupling strength from the phonon side band for Eu^{3+} ions in this glass matrix as discussed later.

The asymmetric emission spectrum of Pr^{3+} in the region

Table 3. Calculated and observed radiative parameters for Pr^{3+}, Eu^{3+} and Dy^{3+} ions in NTZP glass.

Transition	ν (cm^{-1})	A (s^{-1})	β_R (cal)	β_R (obs)	τ_R (μs)	$\sigma_p \times 10^{-22}$ (cm^2)	Ratio of areas
Praseodymium (III)*							
$^3P_0 \rightarrow {}^3H_4$	20534	16885	0·66	0·64 (0·83)	39·4	257	
$^3P_0 \rightarrow {}^3H_5$	18182	—	—	0·08 (0·08)		—	
$^3P_0 \rightarrow {}^3H_6$	16239	4996	0·20	0·24 (0·07)		156	
$^3P_0 \rightarrow {}^3F_2$	15537	3466	0·14	0·03 (0·01)		281	
$^3P_1 \rightarrow {}^3H_5$	19387	11069	0·34	—	30·7	291	
$^1D_2 \rightarrow {}^3H_4$	16726	961	0·41	—	415	—	
Europium (III)							
$^5D_0 \rightarrow {}^7F_0$	17271	—	—	0·03	—		
$^5D_0 \rightarrow {}^7F_1$	16915	—	—	0·28	—	—	
$^5D_0 \rightarrow {}^7F_2$	16329	—	—	0·67	—	—	
$^5D_0 \rightarrow {}^7F_3$	15356	—	—	0·009	—	—	
$^5D_0 \rightarrow {}^7F_4$	14310	—	—	0·008	—	—	
R/O = $({}^5D_0 \rightarrow {}^7F_2)/({}^5D_0 \rightarrow {}^7F_1)$							2·38
Dysprosium (III)							
$^4F_{9/2} \rightarrow {}^6H_{15/2}$	21151	294	0·19	0·58	680	4·3	
$^4F_{9/2} \rightarrow {}^6H_{13/2}$	17666	1008	0·68	0·42		37·8	
$^4F_{9/2} \rightarrow {}^6H_{11/2}$	15133	92	0·06	0·02		—	
$^4F_{9/2} \rightarrow {}^6H_{9/2}, {}^6F_{11/2}$	13136	30	0·02	—		—	
$^4F_{9/2} \rightarrow {}^6H_{7/2}, {}^6F_{9/2}$	11909	25	0·02	—		—	
$^4F_{9/2} \rightarrow {}^6H_{5/2}, {}^6F_{7/2}$	10004	10·6	0·007	—		—	
$^4F_{9/2} \rightarrow {}^6F_{9/2}$	8668	10·1	0·007	—		—	
Y/B = $({}^4F_{9/2} \rightarrow {}^6H_{15/2})/({}^4F_{9/2} \rightarrow {}^6H_{13/2})$							0·71

*Parenthesis values indicate the branching ratios of Pr^{3+} at 77 K.

517–570 nm is composed of a major peak due to $^3P_1 \rightarrow {}^3H_5$ and a minor peak due to $^3P_0 \rightarrow {}^3H_5$ (figure 1). The latter is a strong dipole forbidden transition and its presence indicates significant $J–J$ mixing (Strek *et al* 1985). The relative emission intensities of Pr^{3+} originating from $^3P_1$ level significantly decreases on cooling the sample to 77 K (figure 1). The appearance of $^3P_1$ emission at higher temperature is due to the enhanced Boltzmann population of the higher Stark components of the ground state ($^3H_4$) facilitating direct pumping to $^3P_1$ and/or by the thermal excitation from $^3P_0$ to $^3P_1$ (Strek *et al* 1985). The possible reasons for the disagreement in the observed and calculated branching ratios for $^3P_0 \rightarrow {}^3H_6$ and $^3P_0 \rightarrow {}^3F_2$ may be due to interference of other emission transitions from $^3P_1$ level occurring in the same regions (Nachimuthu and Jagannathan 1995a; Zhao and Flemming 1997).

Eu³⁺: The ground state of $Eu^{3+}(4f^6)$ is $^7F_0$. The excitation spectrum of Eu^{3+} monitored at $^5D_0 \rightarrow {}^7F_2$ shows the

phonon assisted side band for $^5D_2 \leftarrow {}^7F_0$ transition at higher energy side (figure 2). The energy between the pure electronic state and the phonon side band corresponds to the phonon energy, $\hbar\omega$ (Toratoni *et al* 1982). The $\hbar\omega$ value thus obtained (1022 cm⁻¹) is in good agreement with the infrared absorption maximum, $h\nu$ (1024 cm⁻¹), which arises due to the P–O vibrational modes (Videau *et al* 1982; Sobha and Rao 1995b). The value of electron phonon coupling strength ($g = 0.018$), estimated from the ratio of the area under phonon side band and corresponding pure electronic transition is much higher than g-values for fluoride and oxyfluoride glasses. This is due to the strong covalent bonding of rare earth ion with the local site and also higher non-radiative decay could be expected in this glass system (Tanabe *et al* 1992).

The position of $^5D_0 \rightarrow {}^7F_0$ of Eu^{3+} emission is characteristic of the coordination of the Eu^{3+} ion (Boulon *et al* 1985). This emission transition is found to be in the range 17,271–17,574 cm⁻¹ suggesting the 8–9
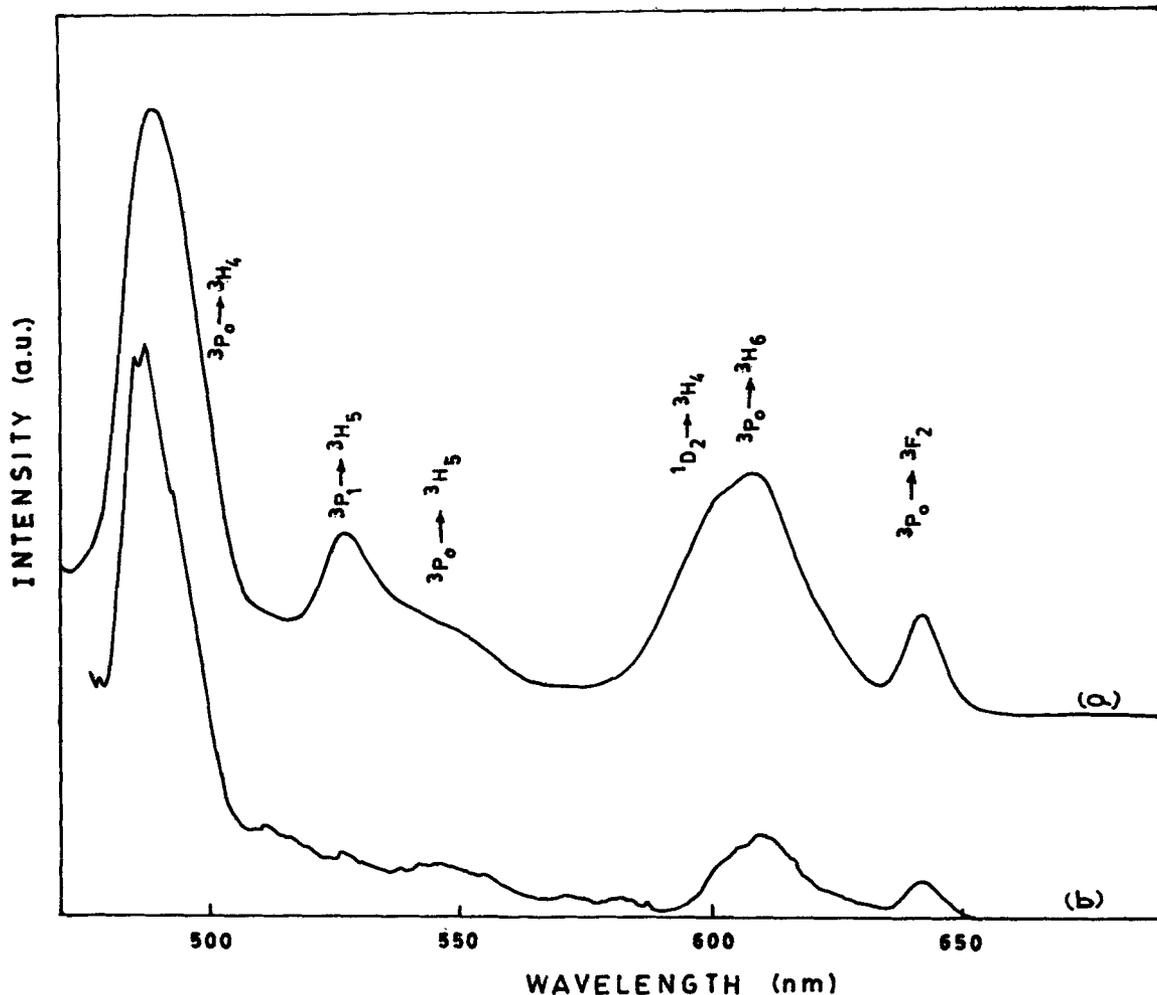

Figure 1. Emission spectra of 2 wt% Pr^{3+} doped NTZP glass excited at 446 nm (a) at room temperature and (b) at 77 K.

coordination for Eu^{3+}. The room temperature emission spectrum of Eu^{3+} doped in NTZP glass did not show transitions in the high energy region (400–520 nm) unlike fluoride, oxyfluoride, germanate and tellurite glasses (Reisfeld 1975; Nachimuthu and Jagannathan 1995b). The high energy transitions are observed if (i) phonon energy maxima for the parent matrices are low and (ii) electron phonon coupling strengths(g) are high. In the case of germanates, tellurites and oxyfluorides, the phonon energy maximum is quite low and even when the coupling strengths are not high, the high energy transitions are observed. In the case of borates for which the phonon energy maximum is high, irrespective of the coupling strengths the high energy transitions are not observed. In the case of lead phosphate glasses, the phonon energy maxima have intermediate values, but the electron–phonon coupling strengths(g) are quite high and therefore the high energy transitions although weak are observed. In the case of NTZP glass, the phonon energy maximum is no doubt intermediate (1024 cm^{-1}) as in the lead phosphate glass but the electron phonon coupling strength also is much less and hence these transitions are not observed.

The emission spectrum shows two prominent transitions viz. $^5D_0 \rightarrow {}^7F_1$ (orange) and $^5D_0 \rightarrow {}^7F_2$ (red) which appeared around 612 nm and 591 nm, respectively. The transition $^5D_0 \rightarrow {}^7F_1$ is purely magnetic dipole and its intensity is not influenced by metal ligand bonding. On the other hand, $^5D_0 \rightarrow {}^7F_2$ which is electric dipole in

nature and hypersensitive, is very much influenced by local factors such as Eu–O covalency and symmetry around Eu^{3+} ion. Their relative intensities (R/O), thus show a systematic change with the nature of the parent glass matrices (Nachimuthu *et al* 1997). The R/O ratio in the present NTZP glass is found to be 2·38 which is considerably higher than the values observed for the fluoride and oxyfluoride glasses but lower than silicate and borate glasses. It is notable that this ratio is approximately equal to the R/O ratio found in calcium phosphate and calcium alumino phosphate glasses (Nachimuthu 1996). Thus the R/O ratio follows the order

silicate > borate > NTZP ≅ phosphate > oxyfluoride.

Dy^{3+}: The ground state of Dy^{3+} (4f^9) is $^6F_{15/2}$. The hypersensitive transition $^6F_{11/2} \rightarrow {}^6H_{15/2}$ of Dy^{3+} at 1·34 μm has potential for fibre amplifiers (Wei *et al* 1994). The values of Judd–Ofelt parameters are significantly higher than the values reported for fluoride and oxyfluoride glasses (Nachimuthu *et al* 1997). Unlike Eu^{3+}, the two dominant emission transitions $^4F_{9/2} \rightarrow {}^6H_{15/2}$ and $^4F_{9/2} \rightarrow {}^6H_{13/2}$ of Dy^{3+} are electric dipole one of which, $^4F_{9/2} \rightarrow {}^6H_{15/2}$ (yellow), is hypersensitive (figure 3) (Nachimuthu *et al* 1997). Su *et al* (1993) have shown that the ratio of hypersensitive to non-hypersensitive emission transitions of Eu^{3+}, ($^5D_0 \rightarrow {}^7F_2$)/($^5D_0 \rightarrow {}^7F_1$) (i.e. R/O) and ($^4F_{9/2} \rightarrow {}^6H_{15/2}$)/
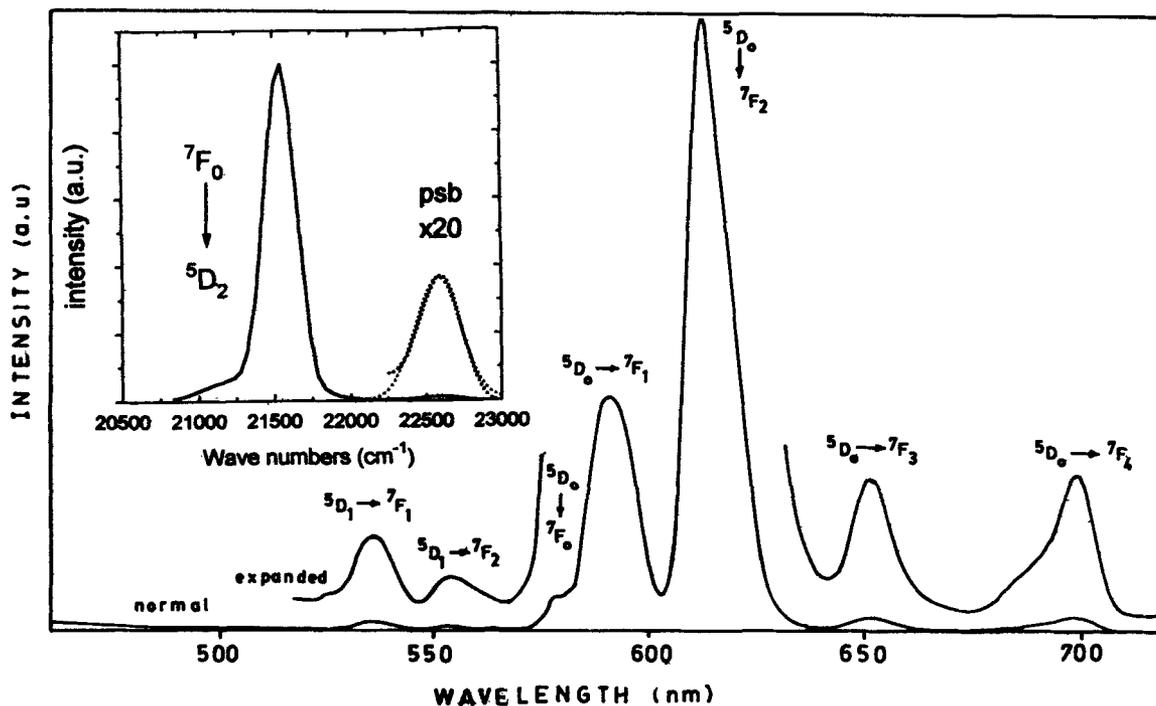

Figure 2. Emission spectrum of 2 wt% Eu^{3+} doped NTZP glass excited at 394 nm. Inset shows the phonon side band (PSB) of Eu^{3+} excitation spectrum monitored at $^5D_0 \rightarrow {}^7F_2$.

$(^4F_{9/2} \rightarrow {}^6H_{13/2})$ (i.e. Y/B) of Dy^{3+} follow a parallel trend as these ratios are sensitive to the covalency and site asymmetry. The emission transitions of Eu^{3+} viz. $^5D_0 \rightarrow {}^7F_1$ and $^5D_2 \rightarrow {}^7F_2$ exhibit strikingly unequal intensity $(R/O = 2.38)$, indicates that the Eu^{3+} ion is predominantly situated in highly distorted asymmetric crystal field. On the other hand, the emission spectrum of Dy^{3+} doped glass shows almost equal intensity $(Y/B = 0.71)$ for two dominant emission transitions $^4F_{9/2} \rightarrow {}^6H_{15/2}$ and $^4F_{9/2} \rightarrow {}^6H_{13/2}$ (figure 3). Su *et al* (1993) have shown that the Y/B ratio for crystalline systems fall in the range 3.0–1.19. Our value lies below this range. This indicates that unlike Eu^{3+} ions, Dy^{3+} ions occupy sites which are less distorted. Such a difference may arise due to significant difference in the radii of (Eu^{3+} 95.0 pm and Dy^{3+} 90.8 pm) the rare earth ions as we go along the lanthanide series.

The Y/B ratio observed for NTZP glass is higher than borate but lower than oxyfluoride, fluoride and silicate glasses. Thus the order of Y/B is

oxyfluoride > silicate $\equiv$ fluoride > NTZP $\equiv$ phosphate
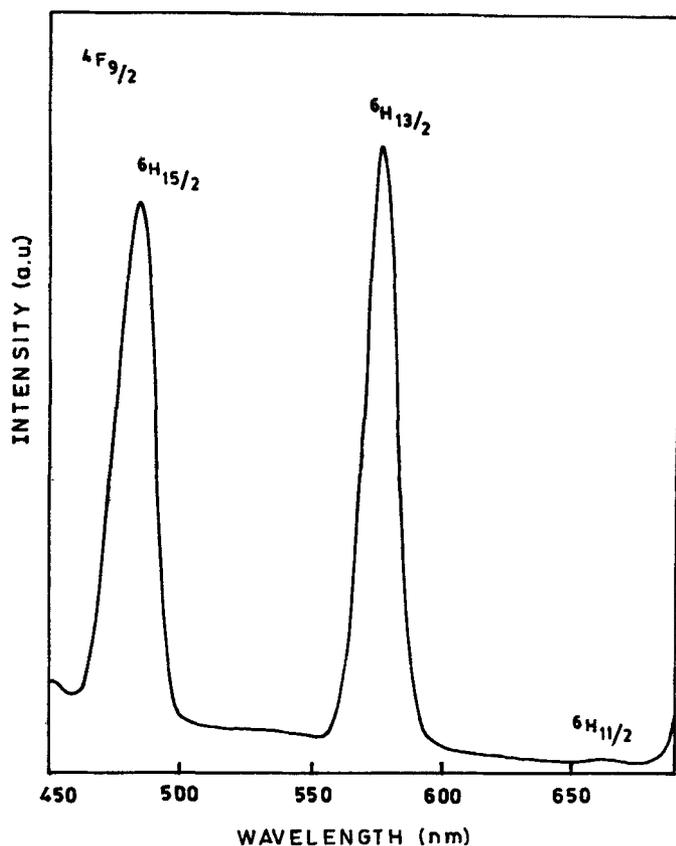> borate.

It is observed that Y/B ratio of phosphate and NTZP glasses are approximately same as the network in both the glasses is closely similar.

The differences in the relative trends of the R/O ratio of Eu^{3+} and Y/B ratio of Dy^{3+} arise due to the differences in the nature of the transition involved. In Dy^{3+} both the transitions are electric dipole, one of which $(^4F_{9/2} \rightarrow {}^6H_{13/2})$ is hypersensitive. Richardson has shown that the intensity calculations of *f–f* transitions in such cases is affected by the differences in charges and polarizabilities of the ligand atoms in the axial and equatorial positions even when the coordination geometries are similar (Richardson *et al* 1981).

The Ω_2 values for Dy^{3+} in NTZP glasses are markedly higher than reported for oxyfluoride and fluoride glasses (Nachimuthu *et al* 1997). This shows that Dy^{3+} is highly covalently bound in these phosphate glass matrices. The radiative parameters for different transitions for Dy^{3+} deduced from Judd–Ofelt parameters are given in table 3. The differences between the calculated and observed branching ratio may arise due to errors involved in determining Ω_λ parameters. However, in view of large number of absorption transitions taken into account and small rms values obtained show that the differences principally arise due to overlapping emissions and non-radiative decay.

5. Conclusions

The Judd–Ofelt parameters deduced from the absorption spectra of Pr^{3+} and Dy^{3+} doped in NASICON type phosphate glass, NTZP give rise to reliable branching ratios for the emission transitions as evidenced by the good matching between the experimental and calculated values. The laser efficiency factors, viz. branching ratios and stimulated emission cross sections of Pr^{3+} doped glass show the potentiality of the glass system as laser medium. The appearance of emission lines from $^3P_1$ level of Pr^{3+} at room temperature are due to thermalization effects. The phonon assisted side band appearing in the Eu^{3+} excitation spectrum is due to P–O vibrational modes. Large electron–phonon coupling strength in this system suggest strong interaction of rare earth ion with the local sites and high non-radiative decay. The emission transition of Eu^{3+}, $^5D_0 \rightarrow {}^7F_0$ is indicative of 8–9 coordination of rare earth with the oxygen ligands. The ratios of hypersensitive to non-hypersensitive emission lines of Eu^{3+} (red/orange) as well as Dy^{3+} (yellow/blue), show that the Eu^{3+} ions are situated in more distorted crystal field compared to Dy^{3+} ions.

Figure 3. Emission spectrum of 2 wt% Dy^{3+} doped NTZP glass excited at 350 nm.

help rendered by Mrs D Usha Rani in preparation of glasses is appreciated.

Appendix

Judd–Ofelt parameters were calculated corresponding to the electronic transitions to the $^3P_0$ level using branching ratios observed from the emission spectrum of Pr^{3+} and the oscillator strength of the $^3H_4 \rightarrow {}^3P_0$ absorption transition according to Bunvel *et al* (1992).

Table. Oscillator strengths and Judd–Ofelt parameters of Pr^{3+} in NTZP glass. The observed values are obtained from absorption and emission spectra.

Pr^{3+} transition	Energy (cm^{-1})	P(10^{-6}) obs	P(10^{-6}) cal
$^3H_4 \rightarrow {}^3F_2$	5197	2·87	2·29
$^3H_4 \rightarrow {}^3F_3$	6554	5·05	6·20
$^3H_4 \rightarrow {}^3F_4$	7092	1·56	3·69
$^3H_4 \rightarrow {}^1G_4$	9038	0·50	0·28
$^3H_4 \rightarrow {}^1D_2$	16926	1·41	1·08
$^3H_4 \rightarrow {}^3P_0$	20734	2·61	2·53
$^3H_4 \rightarrow {}^3P_1$	21267	3·58	3·86
$^3H_4 \rightarrow {}^3P_2$*	22512	7·47	3·62
$^3H_5 \rightarrow {}^3P_0$#	18182	0·37	0
$^3H_6 \rightarrow {}^3P_0$#	16239	1·41	1·17
$^3F_2 \rightarrow {}^3P_0$#	15537	0·19	0·34

$\Omega_2 = 0.40 \times 10^{-20} \text{ cm}^2$

$\Omega_4 = 3.87 \times 10^{-20} \text{ cm}^2$

$\Omega_6 = 5.46 \times 10^{-20} \text{ cm}^2$

rms = 1·42

*hypersensitive transition.
#calculated from emission spectrum of Pr^{3+}.

References

Binnemans K and Gorller-Walrand C 1998 *J. Phys. Condens. Matter* **10** L167

Boulon G, Bouderbala M and Seriot J 1985 *J. Less-Common Metals* **112** 41

Bunvel M A, Cases R, Chamano M A and Alcala R 1992 *Phys. Chem. Glasses* **33** 16

Caird J A, Ramponi A J and Staver P R 1991 *J. Opt. Soc. Am.* **B8** 1391

Carnall W T, Hessler Jan P and Wagner F Jr 1978 *J. Phys. Chem.* **82** 2152

Cho Doo-Hee, Hirao Kazuyki, Fujita Koji and Soga Naohiro 1996 *J. Am. Ceram. Soc.* **79** 327

Durville Frederic M, Behrens Edward G and Powell Richard C 1987 *Phys. Rev.* **B35** 4109

Hagman L and Kierkegaard P 1968 *Acta Chem. Scand.* **22** 1822

Menezes L de S, Cid b de Araujo, Maciel G S, Messadeq Y and Aegerter M A 1997 *Appl. Phys. Lett.* **70** 683

Nachimuthu P 1996 *Optical properties of lanthanide ions doped in borate, phosphate and oxyfluoride glasses*, Ph D thesis, University of Hyderabad, Hyderabad

Nachimuthu P and Jagannathan R 1995a *Phys. Chem. Glasses* **36** 77

Nachimuthu P and Jagannathan R 1995b *Proc. Indian Acad. Sci. (Chem. Sci.)* **107** 59

Nachimuthu P, Jagannathan R, Nirmal Kumar V and Narayana Rao D 1997 *J. Non-Cryst. Solids* **217** 215

Reisfeld R 1975 *Struct. and Bond* **22** 123 and references therein

Richardson F S, Saxe J D, Davis S A and Faulkner T R 1981 *Molec. Phys.* **42** 1401

Sobha K C and Rao K J 1995a *Solid State Ionics* **81** 145

Sobha K C and Rao K J 1995b *Proc. Indian Acad. Sci. (Chem. Sci.)* **107** 573

Sobha K C and Rao K J 1996a *J. Non-Cryst. Solids* **201** 52

Sobha K C and Rao K J 1996b *J. Phys. Chem. Solids* **57** 1263

Srikanth Sarma P R, Jagannathan R and Vithal M 1992 *J. Chem. Soc. Dalton Trans.* 723

Strek W, Szafranski C, Deren P, Jablonski K and Jezowska-Trzebiaatowska B 1985 *Rare earth spectroscopy* (eds) B Jezowska-Trzebiaatowska, J Legendziewicz and W Strek (Philadelphia: World Scientific) p. 340

Su Qiang, Pei Zhiwu, Chi Lisheng, Zang Hongjie, Zhang Zhongyi and Zou Feng 1993 *J. Alloys & Comp.* **192** 25

Tanabe S, Hirao K and Soga N 1992 *J. Non-Cryst. Solids* **142** 148

Toratoni H, Jzumitani T and Kuroda H 1982 *J. Non-Cryst. Solids* **52** 303

Videau J J, Portier J and Pirion V 1982 *J. Non-Cryst. Solids* **48** 385

Vijaya Prakash G, Nachimuthu P, Vithal M and Jagannathan R 1998 unpublished

Wei K, Machewirth D P, Wenzel J, Snitzer E and Sigel Jr G H 1994 *Opt. Lett.* **19** 904

Yzexing Zhao 1995 *Opt. Lett.* **20** 566

Zhao Yuzing and Flemming Simon 1997 *IEEE J. QE* **33** 905